CRYSTAL GROWTH & DESIGN

Article

pubs.acs.org/crystal

Molecular Construction Using $(C_3N_3O_3)^{3-}$ Anions: Analysis and Prospect for Inorganic Metal Cyanurates Nonlinear Optical Materials

Fei Liang,[†,‡] Lei Kang,[†] Xinyuan Zhang,[†] Ming-Hsien Lee,[*,§] Zheshuai Lin,[*,†,‡] and Yicheng Wu[†]

[†]Center for Crystal Research and Development, Key Lab Functional Crystals and Laser Technology of Chinese Academy of Sciences, Technical Institute of Physics and Chemistry, Chinese Academy of Sciences, Beijing 100190, P. R. China

[‡]University of Chinese Academy of Sciences, Beijing 100190, P. R. China

[§]Department of Physics, Tamkang University, New Taipei 25137, Taiwan

Supporting Information

ABSTRACT: Molecular construction using good optically active microscopic units is vital to efficiently explore good nonlinear optical (NLO) materials, a type of important optoelectronic functional materials. In this work, we highlight the planar $(C_3N_3O_3)^{3-}$ anion, the main fundamental building block in inorganic metal cyanurates, as an outstanding candidate of building blocks for NLO materials. Several noncentrosymmetric metal cyanurates containing the $(C_3N_3O_3)^{3-}$ groups are studied by the first-principles calculations for the first time. It is shown that these materials possess wide band gaps (E_g > 5.5 eV), high SHG coefficients (d_{22} > 2 × BBO), and large birefringence values (Δn > 0.1) and thus have good potentials in the ultraviolet NLO applications. Moreover, the key role of the $(C_3N_3O_3)^{3-}$ groups to the good NLO performance in the cyanurates is elucidated. On the basis of the first-principles analysis, some possible searching directions of good NLO materials containing $(C_3N_3O_3)^{3-}$ groups are proposed.

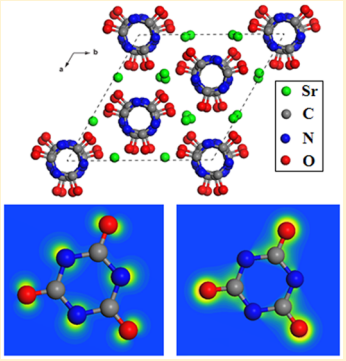

INTRODUCTION

Nonlinear optical (NLO) crystals have very important applications in many advanced scientific and technological fields, such as laser frequency conversion,[1] biological tissue imaging,[2] environmental monitoring,[3] and minimally invasive medical surgery.[4] In the last three decades, the search for NLO materials has made great progress,[5] and some outstanding ultraviolet (UV) and deep-UV inorganic NLO crystals have been discovered, including β-BaB_2O_4 (BBO),[6] LiB_3O_5 (LBO),[7] $CsLiB_6O_{10}$ (CLBO),[8] and $KBe_2BO_3F_2$ (KBBF).[9] In particular, BBO crystal has been used widely in second-, third-, fourth-, and fifth-harmonic generation, as well as in optical parametric oscillators (OPO) and optical parametric amplifiers (OPA),[10] owing to its short UV cutoff edge (190 nm), high transparency from 0.2 to 2.6 μm (T > 50%), high SHG coefficients (d_{22} = 4.1 × KDPd_{36}), large birefringence (Δn = 0.12@1064 nm), and high damage threshold.[6] Recently, BBO crystals have been also used for pairs of entangled photons generation in a quantum information experimental system[11] and micro/nanoscale optical modulation.[12] It is well-known that the excellence of NLO properties in BBO comes from the planar $(B_3O_6)^{3-}$ anions, a typical delocalized π-conjugated anionic group. First-principles calculations demonstrated that the contribution of $(B_3O_6)^{3-}$ units to SHG coefficients for BBO is more than 80%, while to birefringence is more than 85%.[13] This strongly suggests that the molecular construction using large π-conjugated groups would be a very efficient way for searching new materials with good NLO performance.

According to valence bond theory,[14] some key points about large π-conjugated groups should be clarified: (i) all atoms should be in the planar or essentially planar configuration; (ii) all atoms should provide parallel p orbitals by each other; (iii) the number of p electrons should be less than twice the number of conjugated p orbitals; (iv) the overlap between p_π–p_π orbitals should be large as much as possible, which means large electron population of the conjugated π-orbital systems. Note that the large π-conjugated $(B_3O_6)^{3-}$ groups are very rarely found: the planar $(B_3O_6)^{3-}$ units only exist in BBO,[6] KBO_2,[15] $Ba_2Mg(B_3O_6)_2$,[16] $CsZn_2B_3O_7$,[17,18] γ-$KBe_2B_3O_7$,[19] and LiB_6O_9F.[20] This urges us to search other types of large π-conjugated groups as the fundamental building blocks (FBBs) for inorganic NLO materials, especially for those possessing high SHG effect and large birefringence.

On the basis of a thorough survey in the inorganic crystal structure database (ICSD, 2016-2, Version 1.9.8, by Fachinformationszentrum Karlsruhe, Germany), we find that cyclotrinitridoborate $(B_3N_6)^{9-}$, oxonitridoborate $(B_3N_3O_3)^{6-}$, and cyanuric $(C_3N_3O_3)^{3-}$ units are possible candidates.[21−23] Nonetheless, the compounds containing the $(B_3N_6)^{9-}$ unit are usually crystallized in a centrosymmetric space group,[21] and the $(B_3N_3O_3)^{6-}$ unit is distorted from the planar geometric configuration.[22] In comparison, the $(C_3N_3O_3)^{3-}$ anion is formed by three linear $(OCN)^-$ units linked with a cyclic

Received: May 13, 2017
Revised: May 23, 2017
Published: June 1, 2017

DOI: 10.1021/acs.cgd.7b00677
Cryst. Growth Des. 2017, 17, 4015−4020

(C_3N_3) moiety and three exocyclic oxygen atoms,[24] which is isoelectric with $(B_3O_6)^{3-}$ units, and contains large delocalized π-conjugated electron orbitals. Till now, the organic derivatives of cyanuric acid have found many industrial applications, but its inorganic derivatives have not yet been paid wide attention as NLO materials.[24] To the best of our knowledge, only one research group (Meyer et al.) has focused on this system and succeeded in synthesizing several noncentrosymmetric (NCS) metal cyanurates, including $Ca_3(C_3N_3O_3)_2$ (CCY),[25] α-$Sr_3(C_3N_3O_3)_2$ (α-SCY),[26] β-$Sr_3(C_3N_3O_3)_2$ (β-SCY),[27] and $Eu_3(C_3N_3O_3)_2$ (ECY).[27] These metal cyanurates were prepared by oxygen-free high temperature solid-state reactions between metal chlorides and Li(OCN)/K(OCN) at temperatures of around 500 °C.[28] DSC measurements showed that SCY is a congruent melting compound with onset points at 628 °C for melting and 634 °C for recrystallization.[26] Therefore, it is possible to grow large sized SCY crystals by Bridgman methods. In addition, Meyer has given a binary phase diagram of SCY and K(OCN) with different molar ratios, thus suggesting that this simple system with excess K(OCN) can be intended as a flux medium for crystal growth.[29] Especially, CCY, α-SCY, and β-SCY exhibited stronger SHG response than that of BBO under 800 nm irradiations in the primary experiments.[25−27,29] This, actually, implies that the $(C_3N_3O_3)^{3-}$ group, the FBB in metal cyanurates, should be suitable as the outstanding NLO active microscopic unit. However, up to now, the importance of the $(C_3N_3O_3)^{3-}$ group has not attracted attention, and the analysis and prospect of the inorganic metal cyanurates NLO materials is also very lacking.

In this work, we take β-SCY and CCY as the representative examples in the NCS inorganic cyanurates to demonstrate the key role of $(C_3N_3O_3)^{3-}$ anions to their NLO performance. On the basis of the first-principles electronic structure calculations, the optical properties in β-SCY and CCY are obtained, which are in good agreement with the available experimental results. The dominant contribution of $(C_3N_3O_3)^{3-}$ groups to the SHG effect is elucidated by the real-space atom-cutting method and the SHG-density analysis. Moreover, the prospect of the NLO materials containing $(C_3N_3O_3)^{3-}$ groups is discussed.

COMPUTATIONAL METHODS

The CASTEP package[30] is employed to calculate the electronic band structures as well as linear and nonlinear optical properties of the metal cyanurates. The optimized norm-conserving pseudopotentials[31] and GGA-PBE functional[32] are used to simulate ion−electron interactions for all constituent elements and exchange-correlation potential, respectively. A kinetic energy cutoff of 880 eV is chosen with Monkhorst−Pack k-point meshes spanning less than 0.04/Å^3 in the Brillouin zone.[33] The scissors operator correction[34] is adopted to calculated linear and nonlinear optical properties.

The second-order susceptibility $\chi^{(2)}$ and SHG coefficient d_{ij} ($d_{ij} = 1/2\chi^{(2)}$) are calculated using an expression originally proposed by Rashkeev et al.[35] and developed by Lin et al.[13]

$$\chi_{ijk} = \chi_{ijk}\,(\mathrm{VE}) + \chi_{ijk}\,(\mathrm{VH}) + \chi_{ijk}\,(\text{two bands}) \quad (1)$$

where χ_{ijk} (VE), χ_{ijk} (VH), and χ_{ijk} (two bands) denote the contributions from virtual-electron (VE) processes, virtual-hole (VH) processes, and two band processes, respectively. Moreover, the real-space atom-cutting method and the SHG-density analysis developed in our group[36] are used to analyze and elucidate the microscopic origins of optical properties (for more computational method details, see the Supporting Information).

RESULTS AND DISCUSSION

The crystal structures of β-SCY and CCY are isotypic to that of BBO crystallizing with the NCS $R3c$ space group (Figure 1a,b).[25,27] They contain planar $(C_3N_3O_3)^{3-}$ cyanurate rings that

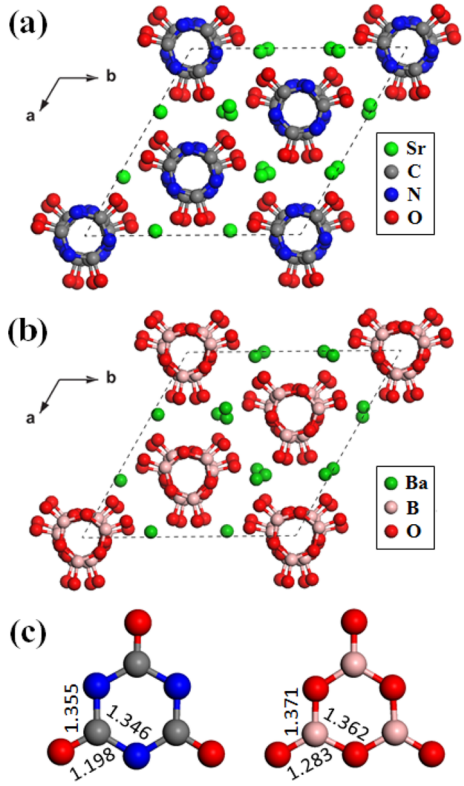

Figure 1. Crystal structures of β-SCY (a) and BBO (b). Comparison of $(C_3N_3O_3)^{3-}$ anions in β-SCY and $(B_3O_6)^{3-}$ anions in BBO is shown in (c).

formed by the cyclic (C_3N_3) moiety and three exocyclic oxygen atoms. There are two crystallographically distinct cyanurate rings in β-SCY, and they are isoelectronic and isostructural to the $(B_3O_6)^{3-}$ units in BBO. These cyanurate anions stack on top of each other along the c-axis to form columns following the similar motif of hexagonal closest packing, whereas alkaline-earth metal cations locate in tunnels between cyanurate columns.

For simplicity, the structure of $(C_3N_3O_3)^{3-}$ groups in β-SCY is discussed in detail as a representative. As shown in Figure 1c, the bond lengths of the $(C_3N_3O_3)^{3-}$ rings in SCY are slightly shorter than those of a cyanuric acid molecule[37] (C−N bonds: 1.37 Å, 1.35 Å; C−O bonds: 1.24 Å), showing a structural change takes place due to ionization. In addition, the interatomic distances in cyanurate rings are shorter than that of oxoborate $(B_3O_6)^{3-}$ anions, indicating the larger overlapping between C 2p, N 2p, and O 2p orbitals, which results in stronger $p_\pi-p_\pi$ interaction in the $(C_3N_3O_3)^{3-}$ anion. Furthermore, the C atom ($2s^22p^2$) has one more electron compared with the B atom ($2s^22p^1$). Therefore, the B atom only provides an empty p_z orbital; otherwise, the C atom can provide a p_z orbital as well as an extra p electron. This is also favorable for obtaining stronger π-conjugated interaction in the (C_3N_3) ring than that in the (B_3O_3) ring. Accordingly, it is expected that the microscopic susceptibility of $(C_3N_3O_3)^{3-}$ groups would be larger than that of $(B_3O_6)^{3-}$ units.

DOI: 10.1021/acs.cgd.7b00677
Cryst. Growth Des. 2017, 17, 4015−4020

The structural parameters of β-SCY, CCY, and BBO are summarized in Table S1, which offers a comparison of our calculated data with experimental results found in the literature. The agreement between the lattice constants calculated in the present work and those from experiments at ambient pressure is very good. It should be noted that the GGA-obtained lattice constant is slightly greater than the experimental values, which is a common observation for this type of calculation. Owing to the larger radius of Sr^{2+}, β-SCY have a larger unit cell volume and lower spatial density of $(C_3N_3O_3)^{3-}$ groups than that of CCY, which thus may lead to some influence on optical properties owing to the "Volume Effect", just as that in the ABBF family (A = K, Rb, Cs).[38]

The GGA electronic band structures of β-SCY and CCY along the lines of high symmetry points in the Brillouin zone are displayed in Figure 2a,c. The valence band maximum

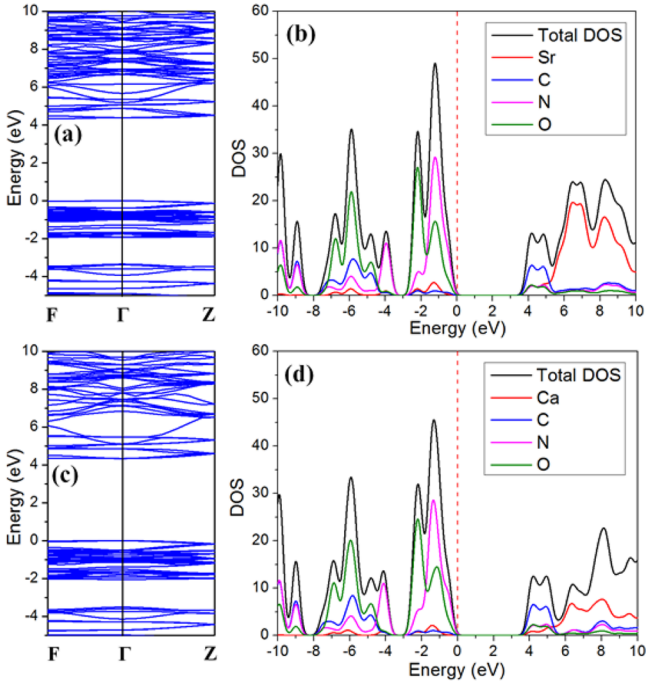

Figure 2. Band structure and total/partial electron density of states of β-SCY (a, b) and CCY (c, d); the red dotted line represents the Fermi level.

(VBM) and conduction band minimum (CBM) positions of β-SCY locate at Γ and F points, respectively, while those of CCY both locate at the Brillouin zone center (Γ point). Accordingly, β-SCY has an indirect band gap, whereas CCY has a direct band gap. The hybrid functionals (HSE06) calculations show that the band gaps in β-SCY and CCY are 5.57 eV (UV absorption cutoff ~ 222 nm) and 5.63 eV (~220 nm), respectively. These values are consistent with the previous density functional theory results that the energy gaps of organic cyanuric acid molecules are 5.53−5.56 eV[39] (for the detailed discussion on band gap calculations, see Table S2). Interestingly, quite a few nonbonding states (i.e., dangling bonds) are presented on the terminal O atoms in $(C_3N_3O_3)^{3-}$ groups. These electronic states can be eliminated by forming the strong covalent bonds with the cations such as B, Be, and Al,[40] and the band gap of the compound can be extended to the deep-UV region (λ_{cutoff} < 200 nm).

The partial density of state (PDOS) projected on the constitutional atoms of β-SCY and CCY is shown in Figure 2b,d and Figure S1. Clearly, the upper part of the VB (−10 to 0 eV) consists of C 2*p*, N 2*p*, and O 2*p* orbitals, and the strong hybridization between oxygen and the neighbor C atoms is exhibited. However, the VBM (−2 to 0 eV) is exclusively occupied by O 2*p* and N 2*p* orbitals. The CBM contains the orbitals of all atoms in β-SCY and CCY while C and O atoms make a major contribution. Since the optical effects of a crystal are mainly determined by the optical transition between the electronic states close to the band gap,[41] it is anticipated that they are dominantly contributed from the $(C_3N_3O_3)^{3-}$ groups. The electron density map (Figure S2) exhibits that the charge densities strongly localize around the $(C_3N_3O_3)^{3-}$ groups, so it is not surprising that the anionic group contributes much more to the optical response than alkaline-earth metal does. In addition, the valency electrons of Sr atoms have obvious overlap with O and C atoms in $(C_3N_3O_3)^{3-}$ groups, while the electron populations of Ca atoms are relatively more local. This can be attributed to large-radius 3*d* orbitals of Sr atoms (Figure S1). Accordingly, we expect that alkaline-earth metal cations will also make a weak influence on optical properties of metal cyanurates.

Taking β-SCY and CCY as examples, they are negative uniaxial crystals because of $n_o > n_e$. The Z dielectric axis is superposed on the *c* crystallographic axis and the XY principal plane is parallel to the *ab* plane. Figure 3 is the dispersion of the

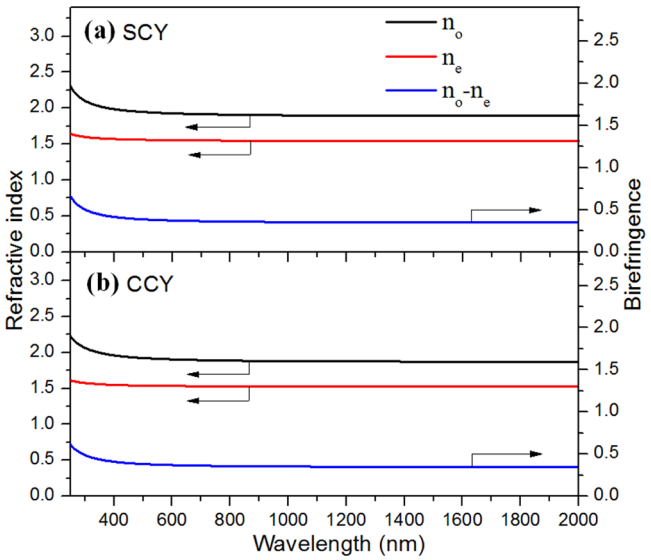

Figure 3. Dispersion of the linear refractive indices for β-SCY (a) and CCY (b) calculated by GGA-PBE functional.

calculated linear refractive indices of β-SCY and CCY. In the region of 250−2000 nm, the calculated birefringence is about 1.20−0.35. In the region of 250−2000 nm, the calculated birefringence is about 1.20−0.35. These birefringence values are much larger than that of BBO (e.g., at 589.3 nm, β-SCY: 0.374, CCY: 0.372 vs BBO: 0.118).[6] The large birefringence is very favorable for achieving the phase-matching condition in the SHG process. Indeed, the shortest phase-matching wavelengths in both β-SCY and CCY can arrive at their UV absorption cutoffs: these compounds are very feasible to generate the fourth-harmonic generation (@266 nm) of a Nd:YAG laser. As one may know, the birefringence value of a crystal is strongly

DOI: 10.1021/acs.cgd.7b00677
Cryst. Growth Des. 2017, 17, 4015−4020

dependent on the anisotropic polarizability. For planar π-conjugated $(C_3N_3O_3)^{3-}$ groups, the out-of-plane polarizability is dominated by delocalized $p_\pi-p_\pi$ orbitals, whereas in-plane polarizability is dominated by sp^2 hybrid σ-bonds between C and N atoms or C and O atoms. Every C and N atom can provide a nonbonding p_z electron, forming into a large π-conjugated orbital, thus resulting in strong anisotropy between the c axis and ab plane.

The birefringence values of β-SCY and CCY are also larger than those of common birefringence crystals, including calcite crystal (0.171@633 nm)[42] and α-BBO (0.122@532 nm),[43] which suggests that metal cyanurates can also be used as a kind of promising material for polarized components applications in the UV region.

According to anion group theory,[44] large NLO effects can be expected in metal cyanurates if the SHG-active $(C_3N_3O_3)^{3-}$ building units occur in high spatial density and coparallel alignment. As measured by Meyer's group, the SHG effect of β-SCY is stronger than that of CCY under the same condition.[29] This is in agreement with our calculated results, in which the d_{22} of β-SCY increases by approximately 10% compared with CCY. In order to analyze the origin of optical properties, the real-space atom-cutting results for the birefringence and SHG coefficients in β-SCY, CCY, and BBO are listed in Table 1,

Table 1. Calculated SHG Coefficients and Birefringence (Δn@1.06 μm) of β-SCY and CCY[c]

	exp	cal (original)	real-space atom-cutting results	
β-SCY			$(C_3N_3O_3)^{3-}$	Sr^{2+}
SHG d_{22}	>BBO[a]	3.93	3.80	1.30
Δn	no data	0.36	0.32	0.081
CCY			$(C_3N_3O_3)^{3-}$	Ca^{2+}
SHG d_{22}	>BBO[a]	3.46	3.45	0.31
Δn	no data	0.35	0.32	0.064
BBO			$(B_3O_6)^{3-}$	Ba^{2+}
SHG d_{22}	±1.6[b]	1.61	1.50	0.36
Δn	0.11[b]	0.12	0.116	0.001

[a]Measured by powder Kurtz–Perry methods.[25,27] [b]Measured by single crystal.[6] [c]The experimental and calculated values of BBO are listed as reference.

from which several conclusions can be summarized: (i) The sum of the SHG coefficients from the respective covalent anions and cations is larger than the original values. This can attributed to unlocal NLO effects, where the total SHG coefficients cannot be considered as the simple summation of contributions from local electronic subsystems.[13] (ii) In the three crystals, the birefringence and SHG coefficient d_{11} dominantly come from the strong planar covalent $(C_3N_3O_3)^{3-}$ or $(B_3O_6)^{3-}$ groups (contribution > 75%). This is in agreement with the conclusions of anion group theory and the strong covalent atomic orbitals close to the band gap in PDOS. (iii) Compared with alkaline metal ions in the ABBF (A = K, Rb, Cs) family,[38] alkaline-earth metal cations make more contribution to optical properties in metal cyanurates because of their higher electron density in VBM and CBM. However, the contributions of the Sr^{2+} and Ca^{2+} cations to SHG coefficients and birefringence are still negligibly small compared with planar $(C_3N_3O_3)^{3-}$ groups.

Moreover, in order to investigate the origin of SHG coefficients visually, the SHG densities of occupied and unoccupied states in SCY are displayed in Figure 4 and Figure S3 as a representative example. The SHG densities of electron

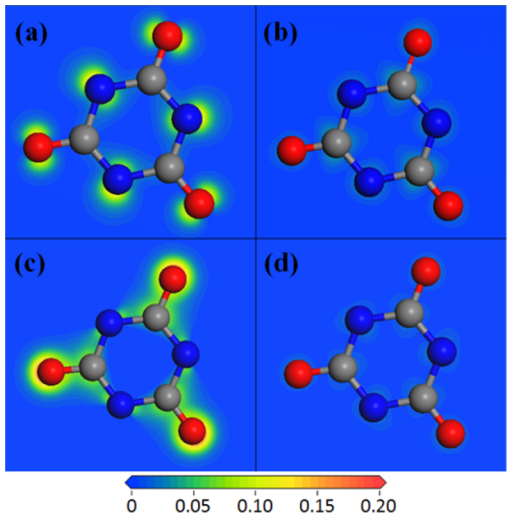

Figure 4. SHG weighted electron densities of β-SCY crystal (a) occupied and (b) unoccupied VE process, (c) occupied and (d) unoccupied VH process along $(C_3N_3O_3)^{3-}$ cross section. The C, N, and O atoms are represented by gray, blue, and red balls, respectively.

states show that the contribution of occupied orbitals to SHG is dominant, while those of unoccupied orbitals are very small. This is consistent with the conclusion in BBO.[36] For the occupied states (Figure 4a), the VE process is mainly originated from the strong hybridization between N and O atomic orbitals in the $(C_3N_3O_3)^{3-}$ groups at VBM. In comparison, the VH process (Figure 4c) primarily comes from the overlap of C and O $2p$ orbitals at CBM. The SHG densities around the alkaline earth cations (Sr^{2+} and Ca^{2+}) are negligibly small, and thus not shown in Figure 4.

On the basis of the above discussion, some opportunities for developing the NLO materials containing $(C_3N_3O_3)^{3-}$ groups seem ready to come out: (i) the trivalent metal cations, such as Y^{3+}, La^{3+}, and Bi^{3+}, are good metal elements for searching new NLO cyanurates. Especially, yttrium cyanurate $YC_3N_3O_3{\cdot}H_2O$ possesses a perfect structural arrangement within the perfect configuration of coplanar $(C_3N_3O_3)^{3-}$ anion units as well as ultrahigh spatial density (see Figure S4).[24] One may find that the cyanurate anion is symmetrically surrounded by three yttrium cations, thus making a large polarization of 2D layers. In addition, attention should be paid to the cyanurate structure similar to 2D organic topological insulators (TIs), such as $Bi(C_6H_5)_3$ and $Pb(C_6H_5)_3$,[45] which may exhibit some exciting optoelectronic properties. (ii) Other functional SHG-active groups could have been also added into the metal cyanurates, such as $(BO_3)^{3-}$, $(B_3O_6)^{3-}$, $(CO_3)^{2-}$, $(NO_3)^{-}$, etc. The combination and cooperation of multiple anions would provide a new way for finding strong SHG response materials. In fact, some successful examples have been provided as the driving inspiration, such as $Ba_2(BO_3)_{1-x}(CO_3)_xCl_{1+x}$,[46] $Pb_7O(OH)_3(CO_3)_3(BO_3)$ (4.5 × KDP),[47] and $Pb_2(BO_3)(NO_3)$ (9.0 × KDP).[48] (iii) The $(C_3N_3O_3)^{3-}$ anion may be considered as a new functional group for organic Terahertz (THz) NLO crystals. It is anticipated that this group would not only exhibit a large band gap, relating to high LDT, but also be more compatible with organic chromophores. If one could combine $(C_3N_3O_3)^{3-}$ anions with the organic ionic groups in the known

DOI: 10.1021/acs.cgd.7b00677
Cryst. Growth Des. 2017, 17, 4015–4020

organic THz crystals, such as methyl pyridine in DAST[49] and DSTMS,[50] some unprecedented semiorganic NLO materials will be expected. (iv) Last, but not least, BBO crystals have been widely used for pairs of entangled photons generation by spontaneous parametric down-conversion in a modern quantum information experimental system.[11] Similarly, SCY and CCY crystals would also have possible applications in coherent entangled photons generation owing to their higher SHG coefficients and larger birefringence compared with BBO.

CONCLUSION

In summary, the *ab initio* calculations have been carried out to investigate the crucial role of $(C_3N_3O_3)^{3-}$ anions in determining the optical properties in organic metal cyanurates. It is shown that these materials have good potentials in the ultraviolet NLO applications owing to wide band gaps (E_g > 5.5 eV), high SHG coefficients (d_{22} > 2 × BBO), and large birefringence values (Δn > 0.1). Good agreement between experimental and theoretical results is obtained. Taking the β-SCY and CCY as examples, the delocalized π-conjugated orbitals of cyanuric anions are highlighted and it makes the main contribution to large SHG effects and strong optical anisotropy (contribution > 75%). The $(C_3N_3O_3)^{3-}$ group can be regarded as an outstanding fundamental building block for the molecular construction, which we believe has important implications for the research and design of new materials with good NLO performances.

ASSOCIATED CONTENT

Supporting Information

The Supporting Information is available free of charge on the ACS Publications website at DOI: 10.1021/acs.cgd.7b00677.

The optimized lattice parameters, electronic band structure, electron density of states, electron density map, and weighted SHG-density of β-SCY and CCY (PDF)

AUTHOR INFORMATION

Corresponding Authors

*E-mail: mhslee@mail.tku.edu.tw (M.-H.L.).
*E-mail: zslin@mail.ipc.ac.cn (Z.L.).

ORCID

Fei Liang: 0000-0002-4932-1329

Notes

The authors declare no competing financial interest.

ACKNOWLEDGMENTS

This work was supported by the China "863" project (No. 2015AA034203) and the National Natural Science Foundation of China under Grant Nos. 91622118, 91622124, 11174297, and 51602318. M.-H.L. is thankful for equipment support from KeyWin. Inc. and Database service of NCHC.

REFERENCES

(1) Petrov, V. *Prog. Quantum Electron.* **2015**, *42*, 1−106.
(2) Mouras, R.; Bagnaninchi, P.; Downes, A.; Elfick, A. *J. Raman Spectrosc.* **2013**, *44*, 1373−1378.
(3) Pushkarsky, M.; Tsekoun, A.; Dunayevskiy, I. G.; Go, R.; Patel, C. K. N. *Proc. Natl. Acad. Sci. U. S. A.* **2006**, *103*, 10846−10849.
(4) Serebryakov, V. A.; Boiko, E. V.; Petrishchev, N. N.; Yan, A. V. *J. Opt. Technol.* **2010**, *77*, 6−17.
(5) Xia, Y. N.; Chen, C. T.; Tang, D. Y.; Wu, B. C. *Adv. Mater.* **1995**, *7*, 79−81.
(6) Chen, C. T.; Wu, B. C.; Jiang, A. D.; You, G. M. *Sci. China, Ser. B* **1985**, *28*, 235−243.
(7) Chen, C. T.; Wu, Y. C.; Jiang, A. D.; Wu, B. C.; You, G. M.; Li, R. K.; Lin, S. J. *J. Opt. Soc. Am. B* **1989**, *6*, 616−621.
(8) Mori, Y.; Kuroda, I.; Nakajima, S.; Sasaki, T.; Nakai, S. *Appl. Phys. Lett.* **1995**, *67*, 1818−1820.
(9) Chen, C. T.; Wang, G. L.; Wang, X. Y.; Xu, Z. Y. *Appl. Phys. B: Lasers Opt.* **2009**, *97*, 9−25.
(10) Nikogosyan, D. N. *Appl. Phys. A: Solids Surf.* **1991**, *52*, 359−368.
(11) Pan, J.-W.; Chen, Z.-B.; Lu, C.-Y.; Weinfurter, H.; Zeilinger, A.; Zukowski, M. *Rev. Mod. Phys.* **2012**, *84*, 777−838.
(12) Qu, G. Y.; Hu, Z. F.; Wang, Y. P.; Yang, Q.; Tong, L. M. *Adv. Funct. Mater.* **2013**, *23*, 1232−1237.
(13) Lin, J.; Lee, M. H.; Liu, Z. P.; Chen, C. T.; Pickard, C. J. *Phys. Rev. B: Condens. Matter Mater. Phys.* **1999**, *60*, 13380−13389.
(14) Pauling, L. *J. Am. Chem. Soc.* **1932**, *54*, 3570−3582.
(15) Schneider, W.; Carpenter, G. B. *Acta Crystallogr., Sect. B: Struct. Crystallogr. Cryst. Chem.* **1970**, *26*, 1189−1191.
(16) Li, R. K.; Ma, Y. *CrystEngComm* **2012**, *14*, 5421−5424.
(17) Zhao, S.; Zhang, J.; Zhang, S.-q.; Sun, Z.; Lin, Z.; Wu, Y.; Hong, M.; Luo, J. *Inorg. Chem.* **2014**, *53*, 2521−2527.
(18) Yu, H.; Wu, H.; Pan, S.; Yang, Z.; Hou, X.; Su, X.; Jing, Q.; Poeppelmeier, K. R.; Rondinelli, J. M. *J. Am. Chem. Soc.* **2014**, *136*, 1264−1267.
(19) Wang, S.; Ye, N.; Li, W.; Zhao, D. *J. Am. Chem. Soc.* **2010**, *132*, 8779−8786.
(20) Cakmak, G.; Nuss, J.; Jansen, M. *Z. Anorg. Allg. Chem.* **2009**, *635*, 631−636.
(21) Orth, M.; Schnick, W. *Z. Anorg. Allg. Chem.* **1999**, *625*, 551−554.
(22) Schmid, S.; Schnick, W. *Z. Anorg. Allg. Chem.* **2002**, *628*, 1192−1195.
(23) Wiebenga, E. H.; Moerman, N. F. *Nature* **1938**, *141*, 122−122.
(24) Seifer, G. B. *Russ. J. Coord. Chem.* **2002**, *28*, 301−324.
(25) Kalmutzki, M.; Strobele, M.; Wackenhut, F.; Meixner, A. J.; Meyer, H. J. *Angew. Chem., Int. Ed.* **2014**, *53*, 14260−14263.
(26) Kalmutzki, M. J.; Dolabdjian, K.; Wichtner, N.; Ströbele, M.; Berthold, C.; Meyer, H.-J. *Inorg. Chem.* **2017**, *56*, 3357−3362.
(27) Kalmutzki, M.; Strobele, M.; Wackenhut, F.; Meixner, A. J.; Meyer, H. J. *Inorg. Chem.* **2014**, *53*, 12540−12545.
(28) Kalmutzki, M.; Stroebele, M.; Meyer, H. J. *Dalton Trans.* **2013**, *42*, 12934−12939.
(29) Kalmutzki, M.; Wang, X.; Meixner, A. J.; Meyer, H.-J. *Cryst. Res. Technol.* **2016**, *51*, 460−465.
(30) Clark, S. J.; Segall, M. D.; Pickard, C. J.; Hasnip, P. J.; Probert, M. J.; Refson, K.; Payne, M. C. *Z. Kristallogr. - Cryst. Mater.* **2005**, *220*, 567−570.
(31) Rappe, A. M.; Rabe, K. M.; Kaxiras, E.; Joannopoulos, J. D. *Phys. Rev. B: Condens. Matter Mater. Phys.* **1990**, *41*, 1227−1230.
(32) Perdew, J. P.; Burke, K.; Ernzerhof, M. *Phys. Rev. Lett.* **1996**, *77*, 3865−3868.
(33) Monkhorst, H. J.; Pack, J. D. *Phys. Rev. B* **1976**, *13*, 5188−5192.
(34) Wang, C. S.; Klein, B. M. *Phys. Rev. B: Condens. Matter Mater. Phys.* **1981**, *24*, 3417−3429.
(35) Rashkeev, S. N.; Lambrecht, W. R. L.; Segall, B. *Phys. Rev. B: Condens. Matter Mater. Phys.* **1998**, *57*, 3905−3919.
(36) Lin, Z. S.; Jiang, X. X.; Kang, L.; Gong, P. F.; Luo, S. Y.; Lee, M. H. *J. Phys. D: Appl. Phys.* **2014**, *47*, 253001.
(37) Wiebenga, E. H. *J. Am. Chem. Soc.* **1952**, *74*, 6156−6157.
(38) Kang, L.; Luo, S.; Huang, H.; Zheng, T.; Lin, Z. S.; Chen, C. T. *J. Phys.: Condens. Matter* **2012**, *24*, 335503.
(39) Prabhaharan, M.; Prabakaran, A. R.; Srinivasan, S.; Gunasekaran, S. *Spectrochim. Acta, Part A* **2015**, *138*, 711−722.
(40) He, R.; Huang, H.; Kang, L.; Yao, W.; Jiang, X.; Lin, Z.; Qin, J.; Chen, C. *Appl. Phys. Lett.* **2013**, *102*, 231904.
(41) Lee, M.-H.; Yang, C.-H.; Jan, J.-H. *Phys. Rev. B: Condens. Matter Mater. Phys.* **2004**, *70*, 235110.

DOI: 10.1021/acs.cgd.7b00677
Cryst. Growth Des. 2017, 17, 4015−4020

(42) Ghosh, G. *Opt. Commun.* **1999**, *163*, 95−102.
(43) Zhou, G.; Xu, J.; Chen, X.; Zhong, H.; Wang, S.; Xu, K.; Deng, P.; Gan, F. *J. Cryst. Growth* **1998**, *191*, 517−519.
(44) Chen, C. T.; Wu, Y. C.; Li, R. K. *Int. Rev. Phys. Chem.* **1989**, *8*, 65−91.
(45) Wang, Z. F.; Liu, Z.; Liu, F. *Nat. Commun.* **2013**, *4*, 1471.
(46) Zhao, J.; Li, R. K. *Inorg. Chem.* **2012**, *51*, 4568−4571.
(47) Abudoureheman, M.; Wang, L.; Zhang, X.; Yu, H.; Yang, Z.; Lei, C.; Han, J.; Pan, S. *Inorg. Chem.* **2015**, *54*, 4138−4142.
(48) Song, J.-L.; Hu, C.-L.; Xu, X.; Kong, F.; Mao, J.-G. *Angew. Chem., Int. Ed.* **2015**, *54*, 3679−3682.
(49) Marder, S. R.; Perry, J. W.; Schaefer, W. P. *Science* **1989**, *245*, 626−628.
(50) Yang, Z.; Mutter, L.; Stillhart, M.; Ruiz, B.; Aravazhi, S.; Jazbinsek, M.; Schneider, A.; Gramlich, V.; Guenter, P. *Adv. Funct. Mater.* **2007**, *17*, 2018−2023.

DOI: 10.1021/acs.cgd.7b00677
Cryst. Growth Des. 2017, 17, 4015−4020